Anal. Chem. **2004,** *76,* 5705−5712

A Microfabricated Device for Subcellular Organelle Sorting

Hang Lu,[†,⊥] Suzanne Gaudet,[‡] Martin A. Schmidt,[§] and Klavs F. Jensen*[,†]

Department of Chemical Engineering, Department of Biology, and Microsystems Technology Laboratory, Massachusetts Institute of Technology, Cambridge, Massachusetts

We report a microfabricated field flow fractionation device for continuous separation of subcellular organelles by isoelectric focusing. The microdevice provides fast separation in very small samples while avoiding large voltages and heating effects typically associated with conventional electrophoresis-based devices. The basis of the separation is the presence of membrane proteins that give rise to the effective isoelectric points of the organelles. Simulations of isoelectric focusing of mitochondria in microchannels are used to assess design parameters, such as dimensions and time scales. In addition, a model of Joule heating effects in the microdevice during operation indicates that there is no significant heating, even without active cooling. The device is fabricated using a combination of photolithography, thin-film metal deposition/patterning, and electroplating techniques. We demonstrate that in the microfluidic devices, mitochondria from cultured cells migrate under the influence of an electric field into a focused band in less than 6 min, consistent with model predictions. We also illustrate separation of mitochondria from whole cells and nuclei as well as the separation of two mitochondrial subpopulations. When automated and operated in parallel, these microdevices should facilitate high-throughput analysis in studies requiring separation of organelles.

Sample preparation for biochemical analysis of protein activity often requires cell lysis, fractionation, and purification of organelles. For example, to assay cytochrome *c* translocation from mitochondria to cytosol during apoptosis in mammalian cells, the cytosolic and mitochondrial fractions have to be isolated. Similarly, to monitor the translocation of steroid hormone receptors from the cytoplasm to the nucleus, a nuclear fraction must be prepared. Current methods of organelle separation, such as density-gradient centrifugation, immunoisolation, or electromigration analysis, typically require many labor-intensive steps and are not suitable for small-sample analysis.[1] Density-gradient centrifugation is robust, but usually requires repeated centrifugations in different buffers to achieve the desired separation.[2] Immunoisolation is highly specific, but it, too, requires multiple steps.[2] Both methods are time-consuming, with steps performed in series and sample loss occurring during handling. In contrast, newer electromigration separation techniques suitable for separation of cells, membranes, proteins, or other biological particles are usually single-step procedures.[1,3] Variants of electromigration separations, including free flow electrophoresis, high-resolution density-gradient electrophoresis, and immune free flow electrophoresis, make use of the different charges of biological particles and macromolecules to achieve separation. These methods require substantial power input resulting from the large voltages and currents and, therefore, require adequate cooling. Furthermore, because of the physical dimensions of these devices, electrophoretic techniques often require long running times and considerable amounts of sample.

For systems biology studies that require large data sets on many components and samples, parallel and automated organelle separation of small samples is desirable. Microfluidic systems, such as DNA separation chips,[4,5] μFACS,[6] micro diffusion sensors,[7] drug delivery chips,[8] and smart valves,[9] have demonstrated superior performance compared to their macroscopic counterparts. Here, we show the use of a microfluidic device that separates and concentrates organelles by micro *i*so*e*lectric *f*ocusing (micro-IEF).

Isoelectric focusing has been widely applied to protein separation, and microscale IEF of proteins as well as other forms of electrophoretic separation of proteins has been demonstrated.[10−12] In IEF, a pH gradient is created by electrolysis of water at the electrodes and, in most commercial buffers, stabilized by ampholytes—amphoteric molecules with a range of isoelectric

* Corresponding author address: 77 Massachusetts Ave. 66-566, Cambridge, MA 02139. Phone: 617-253-4589. Fax: 617-258-8224. E-mail: kfjensen@mit.edu.

† Department of Chemical Engineering.

‡ Department of Biology.

§ Microsystems Technology Laboratory.

⊥ Current address: 513 Parnassus Ave. Room S-1471, UCSF Department of Anatomy, Box 0452, San Francisco, CA 94143-0452.

(1) Pasquali, C.; Fialka, I.; Huber, L. A. *J. Chromatogr., B* **1999**, *722*, 89−102.

(2) Graham, J. M.; Rickwood, D. *Subcellular Fractionation—A Practical Approach*; Oxford University Press: Oxford, 1997.

(3) Canut, H.; Bauer, J.; Weber, G. *J. Chromatogr., B* **1999**, *722*, 121−139.

(4) Harrison, D. J.; Fluri, K.; Seiler, K.; Fan, Z. H.; Effenhauser, C. S.; Manz, A. *Science* **1993**, *261*, 895−897.

(5) Burns, M. A.; Johnson, B. N.; Brahmasandra, S. N.; Handique, K.; Webster, J. R.; Krishnan, M.; Sammarco, T. S.; Man, P. M.; Jones, D.; Heldsinger, D.; Mastrangelo, C. H.; Burke, D. T. *Science* **1998**, *282*, 484−487.

(6) Fu, A. Y.; Spence, C.; Scherer, A.; Arnold, F. H.; Quake, S. R. *Nat. Biotechnol.* **1999**, *17*, 1109−1111.

(7) Hatch, A.; Kamholz, A. E.; Hawkins, K. R.; Munson, M. S.; Schilling, E. A.; Weigl, B. H.; Yager, P. *Nat. Biotechnol.* **2001**, *19*, 461−465.

(8) Santini, J. T.; Cima, M. J.; Langer, R. *Nature* **1999**, *397*, 335−338.

(9) Beebe, D. J.; Moore, J. S.; Bauer, J. M.; Yu, Q.; Liu, R. H.; Devadoss, C.; Jo, B. H. *Nature* **2000**, *404*, 588−590.

(10) Zhang, C. X.; Manz, A. *Anal. Chem.* **2003**, *75*, 5759−5766.

(11) Gottschlich, N.; Jacobson, S. C.; Culbertson, C. T.; Ramsey, J. M. *Anal. Chem.* **2001**, *73*, 2669−2674.

(12) Macounova, K.; Cabrera, C. R.; Yager, P. *Anal. Chem.* **2001**, *73*, 1627−1633.

10.1021/ac049794g CCC: $27.50
Published on Web 08/27/2004

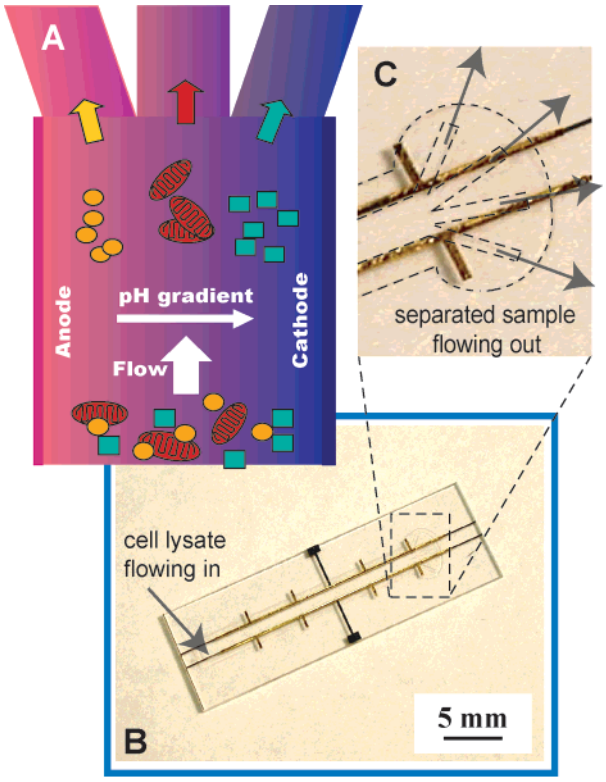

Figure 1. Schematic of field flow isoelectric focusing (IEF) of protein and organelles. (B) Photograph of the microfabricated device before final assembly with (C) enlarged view of the fractionation end of the device. The device consists of electroplated gold electrodes and microfluidic channels formed in a photopatternable epoxy.

points. A protein molecule is mobilized under the influence of the external electric field within this pH gradient and stops migrating when it reaches its isoelectric point (pI), where its net charge is zero (Figure 1). Organelles, which contain many different proteins and other amphoteric molecules on their surfaces, are expected to behave similarly under IEF conditions. However, the time required to focus organelles can be long because of the much larger drag force on organelles than on molecules. The speed at which organelles migrate is proportional to the electric field strength (E) and to their electrophoretic mobility (μ), a function of their size and charge. In conventional IEF systems, molecules or particles traverse the length of the device to focus, typically several tens of centimeters. By considerably shortening the path that the analytes have to traverse, microdevices accelerate focusing.[7] We describe the use of IEF field flow fractionation (FFF) technique in which organelles, specifically mitochondria, migrate in the lateral direction (<1 mm) toward their pIs as they flow longitudinally through the device (cf. Figure 1) to achieve continuous separation of subcellular particles. When coupled with cell lysis and protein identification capabilities, this device should facilitate the studies of complex signal transduction networks.

EXPERIMENTAL SECTION

Model Formulation for Micro Isoelectric Focusing. To aid the design of the microdevice for isoelectric focusing, three models following Mosher and co-workers[13−15] were constructed: (i) a pseudo two-dimensional model for molecular IEF, (ii) a pseudo two-dimensional model for mitochondrial IEF, and (ii) a full three-dimensional (3-D) model for mitochondrial IEF. All forms of the amphoteric species in the bulk solution were described using a reaction-diffusion model. The particular formulation of the problems was chosen to take advantage of the existing solver in FEMLAB (Comsol, Inc., Burlington, MA).

Modeling of molecular IEF served as a benchmark study for estimating the time scale for pH gradient formation and validation the model formulation. The mobility of small ions and molecules were assumed to be constants, and acid−base reactions were incorporated in the transport equations. For example, eqs 1 and 2 described the reactive transport of H^+ and OH^-.

$$v_z \frac{\partial C_H}{\partial z} = \mu_H E \frac{\partial C_H}{\partial x} + D_H \frac{\partial^2 C_H}{\partial x^2} - k_1 C_H C_{OH} + k_2 \quad (1)$$

$$v_z \frac{\partial C_{OH}}{\partial z} = -\mu_{OH} E \frac{\partial C_{OH}}{\partial x} + D_{OH} \frac{\partial^2 C_{OH}}{\partial x^2} - k_1 C_H C_{OH} + k_2 \quad (2)$$

v_z is the fluid velocity calculated from flow rate, μ is the electrophoretic mobility, E is the electric field strength, and k_i's are the reaction constants. C_H and C_{OH} are the concentrations of H^+ and OH^-, respectively. z represents the length along the channel in the stream-wise direction, and x is the cross channel position. Other species (buffer molecules and proteins) were described using analogous equations. A model ampholyte solution was assumed since exact characterization of commercial ampholyte solutions was not available. The ampholyte species used in our experiments were low molecular weight polyaminopolycarboxylic acids and were modeled as protein/peptide molecules with similar characteristics. The physical parameters were either extracted from literature[14] or estimated using liquid-phase reaction kinetics theory.[16] These transport equations were converted to a one-dimensional pseudo time-dependent problem, substituting z/v_z with the time variable.[15] Simulations (detailed in the results section) demonstrated that the time scale for pH gradient establishment is short, on the order of 20 s, and established pH gradient could therefore be assumed in simulations of mitochondria IEF.

To describe the motion of the mitochondria, we constructed a lumped model that includes the electrophoretic mobility of mitochondria as well as their diffusion in two dimensions. The electrophoretic force due to the external electric field, drag force, and Brownian motion are responsible for the movement of the mitochondria. In the equation

$$v_z \frac{\partial C}{\partial z} = -\mu E \frac{\partial C}{\partial x} + D \frac{\partial^2 C}{\partial x^2} \quad (3)$$

v_z is again the average fluid velocity calculated from flow rate, μ is the electrophoretic mobility of the mitochondria as a function

(13) Bier, M.; Palusinski, O. A.; Mosher, R. A.; Saville, D. A. *Science* **1983**, *219*, 1281−1287.
(14) Mosher, R. A.; Dewey, D.; Thormann, W.; Saville, D. A.; Bier, M. *Anal. Chem.* **1989**, *61*, 362−366.
(15) Mosher, R. A.; Saville, D. A.; Thormann, W. *The Dynamics of Electrophoresis*; VCH Publishers: Weinheim, New York, 1992.
(16) Steinfeld, J. I.; Francisco, J. S.; Hase, W. L. *Chemical Kinetics and Dynamics*, 2nd ed.; Prentice Hall: Upper Saddle River, New Jersey, 1999.

of local pH value in the solution, and D is the diffusivity of the particles due to Brownian motion. The electrophoretic mobility of mitochondria from rat kidney extracted from a series of electrophoresis experiments[17] was fit to a third-degree polynomial as a function of pH. The diffusivity of the particles was estimated using the Stokes−Einstein approximation.

$$D = \frac{k_B T}{6\pi\eta a} \tag{4}$$

η is the viscosity of water; k_B is the Boltzman constant; T was taken as room temperature (300 K); and a was the approximate size of the mitochondria particles, taken as 100 nm. Again, the model was formulated as a pseudo-time-dependent problem by substituting z/v_z with t.

Finally, we constructed a three-dimensional model to examine the effect of the parabolic velocity profile of the pressure-driven flow in the device on the concentration profile. The model incorporated a full 3-D Navier−Stokes calculation on the velocity profile and used the velocity profile in the mass conservation equation.

$$\underline{v}\cdot\underline{\nabla}C = -\mu\underline{E}\cdot\underline{\nabla}C + D\underline{\nabla}\cdot\underline{\nabla}C \tag{5}$$

A linear pH gradient was assumed in the x direction, and the mobility was a function of pH. Because the migrating species was dilute in the buffer solution, the Navier−Stokes equations could be decoupled from the mass conservation equations, solved first, and the resulting velocity profile then used as input to the species simulations.

Fabrication of Microfluidic Devices. Pyrex 7740 wafers (Bullen Ultrasonic Inc.) were cleaned in a bubbling piranha solution (1:3 sulfuric acid and hydrogen peroxide) for 10 min. (**Caution:** *The mixing process is strongly exothermic and releases hot vapor, and the mixture is highly reactive. Personal protective wares including face shield, apron, and gloves should be used.*) The wafers were rinsed in deionized water and dried in a wafer spin dryer. The wafers were then treated with hexamethyldisilazane (HMDS) vapor and coated with image reversal resist AZ5214-E (Clariant Corp., Somerville, NJ). The image reversal resist was patterned using standard photolithography techniques (brief exposure through the metal seed-layer mask followed by a flood exposure) and developed. A thin film of gold (2000 Å) with titanium as an adhesion layer (100 Å) was deposited in an electron-beam evaporator. The metal seed-layer pattern was formed in a lift-off process in which the photoresist was removed in solvent along with the metal film deposited on top of it, leaving metal only in open regions of the original photoresist pattern. Subsequently, a layer of a photopatternable epoxy SU-8-50 (MicroChem Corp., Newton, MA) was spun and patterned using photolithography to create the trenches in which the gold electrodes were to be formed. The current supplied to the substrates controlled the gold deposition rate; generally, to plate 50-μm-thick electrode required 4−5 h at 60 °C using a noncyanide-based plating solution (Technic Inc., Cranston, RI). At the completion of electroplating, the SU-8-50 mold was removed in a Nanostrip solution (Cyantek Corp., Fremont, CA). The wafers were rinsed and dried before cleaning in oxygen plasma for at least 30 min.

To form the flow channels of the devices, another layer of SU-8-50 was coated and patterned. The wafers were coated with a layer of thick resist AZ4620 (Clariant Corporation, Fair Lawn, NJ) to protect the features before they were diced into individual devices using a Disco dice saw and solvents (acetone, ethanol, followed by isopropyl alcohol) were used to remove the thick photoresist. Fluidic access holes on the glass substrate were drilled using a 0.75-mm diamond drill bit. The device was capped by a microscope coverslip sealed by epoxy on the edges. Conductive epoxy (SPI Supplies, West Chester, PA) was used to bond wires to the thin-film gold contact pads on the glass substrate.

Cell Culture and Lysate Preparation. HT-29 cells (human colon carcinoma, ATCC, Manassas, VA) and HeLa cells (ATCC, Manassas, VA) were cultured in McCoy's 5A and DMEM medium, respectively, supplemented with 10% fetal serum, 100 units/mL penicillin, 100 μg/mL streptomycin, and 2 mM glutamine (Invitrogen, Carlsbad, CA) at 37 °C and 5% CO_2. NR6wt murine fibroblasts (ATCC, Manassas, VA) were cultured in MEMα with 7.5% fetal serum, 350 μg/mL G418, 1 mM sodium pyruvate, 2 mM L-glutamine, 1 mM nonessential amino acids, 100 i.u./mL penicillin, and 200 μg/mL streptomycin (Invitrogen, Carlsbad, CA) under the same conditions. For the experiment using apoptotic cells, HeLa cells were treated with 50 ng/mL TNF (Peprotech, Rocky Hill, NJ) and 2.5 μg/mL cycloheximide (Sigma-Aldrich, St. Louis, MO). The floating cells were collected after 4 h.

The mitochondria were labeled in live cells with 500 nM MitoTracker Green or 5 μg/mL JC-1 (Molecular Probes Inc., Eugene, OR) at 37 °C for 30 min. The cells were harvested with 0.25% trypsin and 1 mM EDTA (Invitrogen, Carlsbad, CA).

To label peroxisomes with GFP, we prepared a construct driving the expression of EGFP with the Ser-Lys-Leu peroxisome targeting signal added to its C terminus. The modified EGFP was expressed under the CMV promoter in the pcDNA3.1+ vector (Invitrogen, Carlsbad, CA). HeLa cells were transiently transfected with this construct using Fugene 6 as directed by the manufacturer (Roche Molecular Biochemicals, Basel, Switzerland). The cells were collected 24 h after transfection.

To prepare cell lysates and mitochondria fractions, cells were rinsed in cold PBS followed by cold MB-EDTA buffer (10 mM HEPES pH 7.3, 1 mM EDTA, 210 mM mannitol, 70 mM sucrose, 250 μM PMSF, 10 μg/mL leupeptin, 10 μg/mL pepstatin, and 10 μg/mL chymostatin, all reagents from Sigma-Aldrich, St-Louis, MO). The cells were then swollen in MB-EDTA buffer for 10 min on ice and sheared through a 26G needle. The nuclei were labeled using 200 nM propidium iodide (Molecular Probes Inc., Eugene, OR) added to the lysate. In the experiments in which mitochondria were focused directly in the lysate, this fraction was used. For isoelectric focusing of the crude mitochondria fraction, the lysate was centrifuged at 2000g for 2 min, and the supernatant was then centrifuged at 13000g for 10 min at 4 °C to sediment the mitochondria. This second pellet, resuspended in MB-EGTA buffer (same as MB-EDTA except EDTA was replaced with 1 mM EGTA) constituted the crude mitochondria fraction.

IEF and Microscopy. The microfabricated device was mounted on a Zeiss Axiovert200 fluorescence microscope with an ORCA-

(17) Plummer, D. T. *Biochem. J.* **1965**, *96*, 729.

100 cooled digital camera (Hamamatsu, Bridgewater, NJ). Before each experiment, the device was first flushed with bleach (1−2 mL) and rinsed with ∼5 mL of water and ∼3 mL of PBS. A bovine serum albumin solution (5% w/v in water, ∼3 mL) was flushed through the device and incubated for 20 min to passivate the device walls. For IEF experiments, Ampholine pH 3−6 or pH 3−10 buffer solution (Amersham Biosciences, Piscataway, NJ) was added to a final concentration of 2%. The ∼2-V DC voltage was supplied using Protek 3015B, and the current was steadied at ∼30 μA. Fluid was delivered by a syringe pump (Harvard Apparatus, Holliston, MA).

RESULTS

Design Considerations. Available large-scale devices usually take a few hours[3,18,19] to achieve the separation of proteins. The rate at which proteins move is proportional to the fixed field strength and their electrophoretic mobility. Larger entities, specifically organelles, will focus even more slowly owing to the much larger drag force on the particles than that on protein molecules. In conventional macrosystems, proteins of interest have to traverse the width of the device (a few centimeters) to focus. Microscale devices can considerably shorten the time required for focusing by shortening the path that the particles travel. The voltage required to maintain a similar electric field is correspondingly smaller. Finally, the device effluent containing focused streams of organelles can be separated into fractions by taking advantage of laminar flow properties of microfluidic devices.

There are three important time scales to consider in the design of micro IEF devices: electrophoretic mobility, diffusion, and residence time in the device (closely related to the volumetric flow rate of the carrying fluid). Electrophoretic and diffusion effects balance at equilibrium. The field strength and characteristics of the particles of interest define the width of the separated bands. The device should be sufficiently long and narrow to allow enough time for the electrophoretic focusing of the particles. However, making the device too narrow will compromise the resolution of the separation.

Modeling Isoelectric Focusing of Mitochondria. Bier et al. introduced models to simulate pH gradient formation processes[13] in which the pH gradient is stabilized by a few amphoteric species (such as amino acids) with known charge states and mobility. We carried out a simulation of pH gradient formation (prefocusing) to examine the time scale during which it would take place in microdevices. We used a 1-dimensional pseudo time-dependent model solved in FEMLAB, applying a method adapted from Mosher et al.[13,15] All forms of amphoteric species in the solution were described with a reaction−diffusion model. Figure 2A describes the simulation results. At the beginning of the simulation (equivalent to the inlet of the channel), molecules were uniformly distributed throughout the channel in the *x* direction. As time progressed (or as the analytes flowed through the device in the *z* direction), a peak in the concentration distribution started to develop, and eventually reached steady state. For a 2-V potential across a 1-mm-wide microfluidic device, the time scale for prefocusing was ∼20 s in contrast to typical macroscale IEF, which requires at least 30 min at 1000 V.[19]

(18) Amersham-Biosciences, 2002.

(19) Righetti, P. G. *Isoelectric Focusing: Theory, Methodology and Applications*; Elsevier Biomedical Press: Amsterdam, 1983.

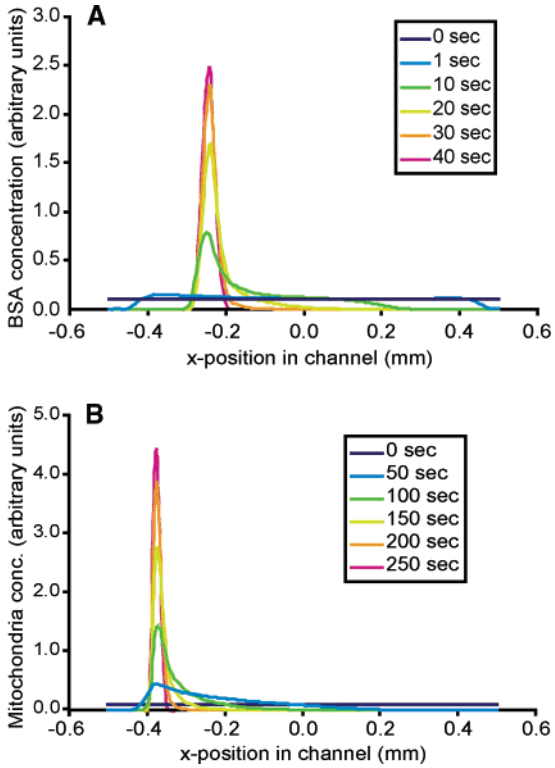

Figure 2. (A) Pseudo two-dimensional simulations of micro-IEF of bovine serum albumin (BSA); (B) Pseudo two-dimensional simulations of micro-IEF of mitochondria from rat liver/kidney cells.

To simulate IEF of mitochondria in the microfluidic device, we constructed a lumped model based on an effective electrophoretic mobility and diffusion coefficient. Mitochondrial IEF behaves very similarly to molecular IEF (see Figure 2B), except time scales for focusing are longer, the concentration peak develops more slowly (∼4 min) and with greater left−right asymmetry, and the peak is narrower at steady state. All of these differences are attributable to smaller electrophoretic mobility and diffusion coefficient of mitochondria, as compared to molecules. On the microscale, Brownian diffusion and, consequently, temperature appear to have a significant impact on the width of the particle concentration distribution. This simulation further demonstrates that pH prefocusing is much faster than mitochondria focusing, and an established pH profile is consequently assumed in subsequent models.

Last, we constructed a three-dimensional (3-D) model to examine the effect of the interplay among diffusion, electrophoretic force, and velocity profile of the pressure-driven flow on the concentration profile (Figure 3). The 3-D model incorporated a full 3-D Navier−Stokes calculation on the velocity profile used in the mass conservation equation. Compared to the pseudo-2D model, the full simulation gives the same time scale for mitochondria focusing (∼4 min), indicating that in devices with large aspect ratio (width/height), a 2-D approximation is adequate and the nonlinear flow profile has minimal effect on the focusing time. Brownian motion of the particles is unimportant when the local concentration of mitochondria is low (e.g., near the inlet of the channel), but is important when the mitochondria are focused. In fact, Brownian diffusion balances the electrical force at steady state, and together they determine the concentration distribution of the focused stream, in qualitative agreement with predictions

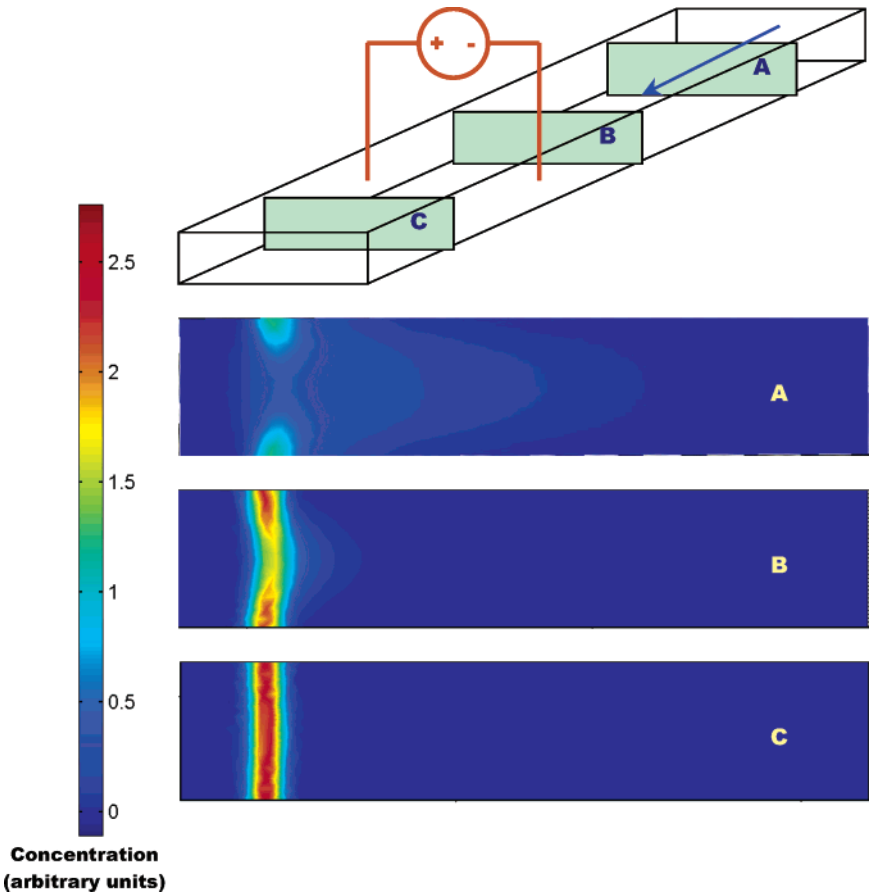

Figure 3. Three-dimensional simulation of the micro-IEF of mitochondria. The color band represents the mitochondria concentration, with red being the highest concentration.

by the 1-D pseudo time model. Moreover, the cross-sectional plots shown in Figure 3 reveal that instead of a butterfly effect in the concentration profile,[20,21] the top and bottom of the velocity field are more focused than the middle owing to the longer residence time at these positions (a result of the parabolic velocity profile).

Focusing Prepared Mitochondrial Fractions. To investigate whether mitochondria exhibit amphoteric surface characteristics under IEF experimental conditions and can be focused in a microfabricated device, an experiment was performed with MitoTraker-labeled HT-29 cell lysate, enriched in mitochondria by differential centrifugation. The sample was delivered by pressure-driven flow. Using a ~2-V applied potential, the mitochondria were focused in the channel under flow condition (Figure 4). When the mitochondria fraction was first introduced into the device, the mitochondria were present throughout the width of the focusing channel (Figure 4, top). As they flowed through the channel, the pH gradient developed, and focusing of mitochondria started to take place (Figure 4, middle). At a residence time of ~6 min (adjusted by varying the flow rate), mitochondria focused near the exit of the channel (Figure 4 bottom). Assuming a linear pH gradient, the mitochondrial focusing position corresponds to a pI value between 4 and 5. These experimental results match well the evolution of the concentration profile obtained from the above simulations (Figure 2B) based on electromobility data from rat kidney mitochondria (~4-min focusing time). Compared to conventional methods of organelle preparation, this microscale IEF is 2 orders of magnitude faster. The separation conditions could, in principle, be fine-tuned for particles of interest and widths of the focused bands by varying flow rate (i.e., residence time in the device) and by using different ampholyte solutions.

Focusing and Concentrating Organelles from Cell Lysate. The separation of mitochondria directly from crude cell lysate provides a validation of the application of the technique as a separation component in an integrated device for subcellular analysis. In a focusing experiment using a mixture of whole cell lysate and intact cells, mitochondria were focused (in effect, enriched and separated from cytosolic materials of signicantly different pIs) in the presence of membrane debris, other organelles, and intact cells (Figure 5). Intact cells were visible, because they contained labeled mitochondria. They migrated toward the anode because of the acidic character of the plasma membrane. In the pH 3−6 range used in this experiment, the cell membrane always carries negative charges.

To further validate the method with a different cell type and compare mitochondria to other organelles, a similar experiment was performed with crude lysate from NR6wt murine fibroblasts cells. In this case, both mitochondria and nuclei were labeled. The mitochondria from NR6wt cells again formed a tightly focused band, clearly separated from nuclei, which migrated to the lower pH side of the device (Figure 6). Nuclei were not as efficiently focused as mitochondria, most probably because their larger size

(20) Kamholz, A. E.; Yager, P. *Biophys. J.* **2001**, *80*, 155−160.
(21) Ismagilov, R. F.; Stroock, A. D.; Kenis, P. J. A.; Whitesides, G.; Stone, H. A. *Appl. Phys. Lett.* **2000**, *76*, 2376−2378.

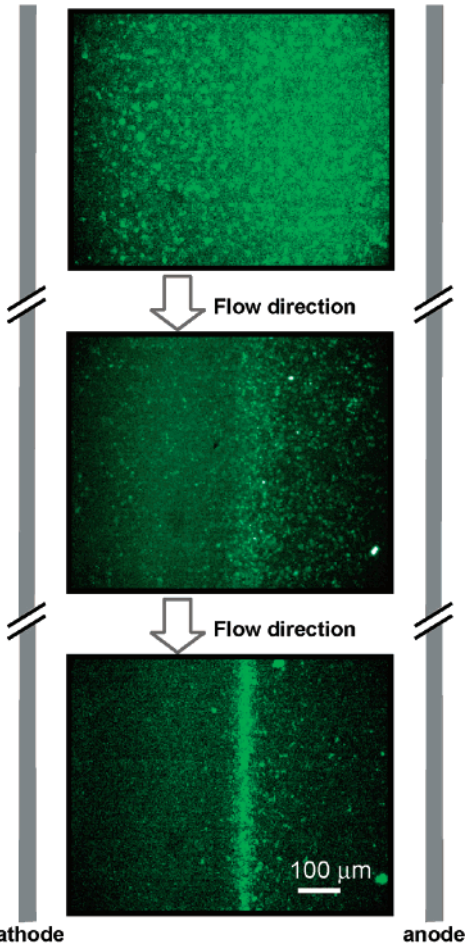

Figure 4. IEF of crudely purified mitochondrial fraction from lysate of HT-29 cell stained with MitoTracker Green. Top views of three different sections of the channel at ~1, 6, and 18 mm from the inlet show that when mitochondria first flow into the channel, their distribution is relatively homogeneous (top). Further along the channel, some focusing is apparent (middle) and close to the exit of the device, the mitochondria form a narrow band (bottom). The electric field is applied laterally. The position of the electrodes is schematic, not to scale. A 3−6 pH buffer range was used; the mitochondria focus at a pI between 4 and 5 (assuming a linear pH profile). The difference in appearance of mitochondria in this and subsequent figures (Figure 5−8) is a result of variations in optical microscopy and experimental conditions.

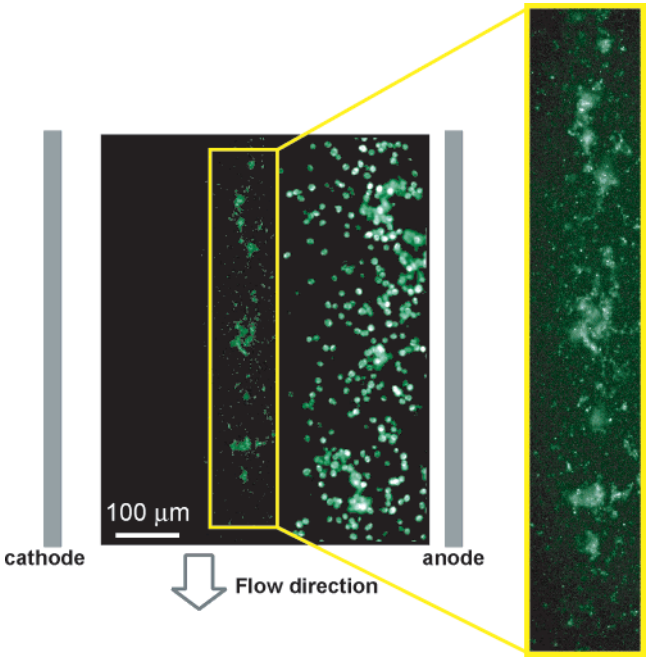

Figure 5. IEF of mitochondria from whole lysate of HT-29 cells stained with MitoTracker Green. Mitochondria focus as well as in their purified form, while intact cells are attracted to the anode because of their negative surface charges under the experimental condition. A pH 3−10 ampholyte buffer range was used; the mitochondria focused at pI between 4 and 5.

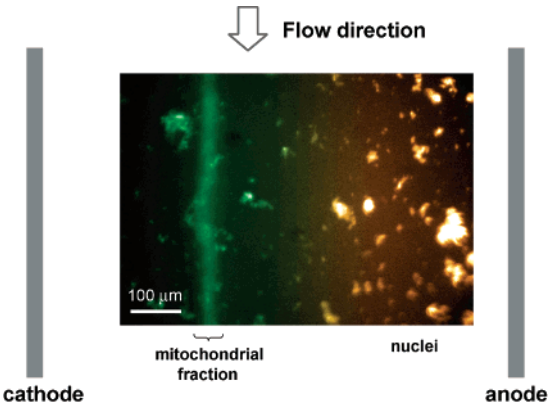

Figure 6. IEF of mitochondria from lysate of NR6wt cells stained with MitoTracker Green and propidium iodide. The mitochondria focus into a distinct narrow band while the nuclei migrate to a broad band. A pH 3−6 buffer was used; the mitochondria focused at pI between 4 and 5.

would require a longer residence time for focusing. It is also possible that the nuclei had a nonuniform isoelectric point. Nonetheless, the mitochondria fraction was free of nuclear contamination, as determined by fluorescence microscopy (Figure 6). Optimization of the microIEF conditions (pH range, residence time, or buffer conditions) could potentially improve focusing of the nuclei fraction.

We used HeLa cells labeled with MitoTraker-Red and transiently transfected with GFP carrying a peroxisome localization signal in experiments exploring separation of mitochondria and peroxisomes. Both organelles could be focused and effectively concentrated, but they comigrated in the electric field (Figure 7). Therefore, to separate these two particular types of organelles, they would first have to be differentiated by modification of their physical or biochemical properties, for example, by binding of antibodies modifying the effective pI.

Despite the different sample treatments (e.g., cell lysis and density centrifugation) under various buffer conditions, the position of the focused mitochondria fractions from these experiments (Figures 4−7) was consistent, all between pH 4 and 5. The mitochondria from the prepared suspension (Figure 4) gave a cleaner appearance, likely due to the absence of soluble and suspended species (e.g., protein, membrane fragments, and debris). In cases in which cleaner fractions or more resolved separations are needed, another microIEF stage with shallower gradient can be used in conjunction of the present device.

Mitochondria Maintain Transmembrane Potential during IEF. We used potential-sensitive dye JC-1[22] to stain the mitochondria and evaluate whether the separation process affects their integrity. The formation of J-aggregates of carbocyanine dyes has

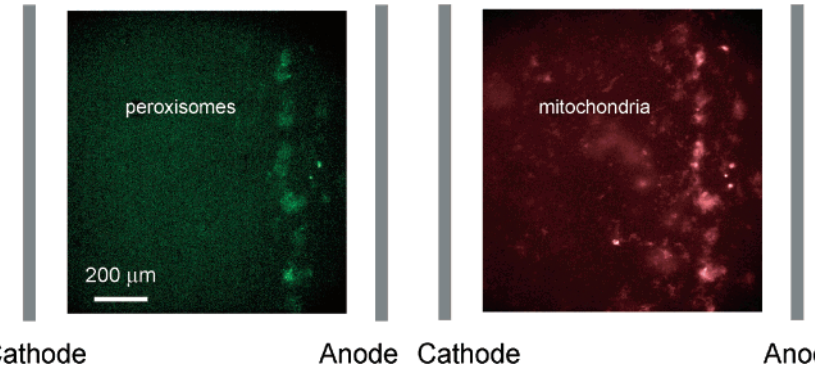

Figure 7. IEF of mitochondria and peroxisomes from HeLa cell lysate. The peroxisomes tagged with GFP and the mitochondria stained with Mitotracker Red migrate to similar pH values, indicating that the two organelles may have similar pIs that do not allow their separation using IEF. However, the two organelles were both effectively enriched in the IEF process. The position of the electrodes is schematic, not to scale. Buffers with a pH range of 3−6 were used.

been shown to be a quantitative fluorescent indicator of mitochondria membrane potential.[22,23] Mitochondria that retain their membrane potential accumulate the dye with subsequent formation of J-aggregates and exhibit mostly red fluorescence (excitation maximum, 535 nm; emission maximum, 590 nm), whereas mitochondria that lose their membrane potential exhibit mostly green fluorescence corresponding to the monomer (excitation maximum, 485 nm; emission maximum, 530 nm). In a micro-IEF experiment using whole cell lysate of JC-1-stained HeLa cells, a strong signal is observed in the red channel throughout the separation process, showing that the mitochondria mostly remain intact in the micro-IEF device (Figure 8A). A weaker signal in the green channel at a different pI close to neutral pH (Figure 8A) is attributed to the small fraction of mitochondria that have lost their membrane integrity during the preparation of the lysates.

The different pIs for intact and compromised membrane potential mitochondria suggest that the device could potentially be used to assay fractions of mitochondria that lose membrane potential when cells undergo apoptosis. Indeed, in a preliminary experiment, HeLa cells were treated with TNF and cycloheximide to induce apoptosis, and the floating cells (committed to apoptosis) were stained with JC-1. Their mitochondria were processed in the micro-IEF device. The fluorescence signals in both the green and red channels for the treated cells were enhanced near neutral pH, as compared to that observed with untreated cells, indicating a higher percentage of the mitochondria with compromised cross-membrane potential in the apoptotic population (Figure 8B). With careful control and calibration, it might be possible to develop a quantitative assay of the extent of mitochondrial potential loss during apoptosis, using this device in conjunction with a potential sensitive dye.

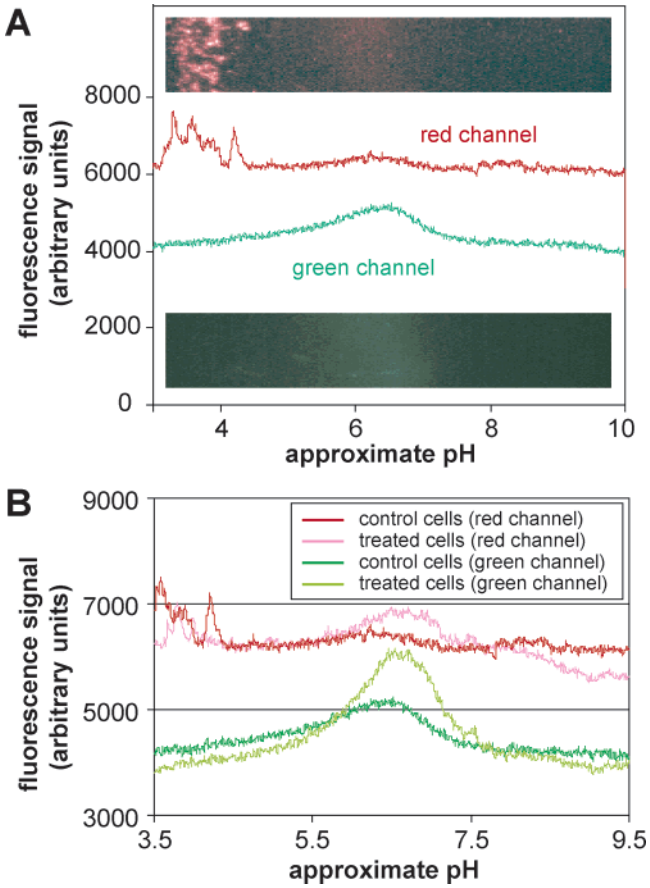

Figure 8. (A) IEF of JC-1 labeled mitochondria from control HeLa cells showing two subpopulations of the organelles. The majority of the mitochondria have a relatively acid pI (mostly visible in the red fluorescence channel), while a small population of mitochondria is near neutral pH (mostly visible in the green fluorescence channel). (B) IEF of JC-1-labeled mitochondria from apoptotic HeLa cells showing larger signals (in both red and green channels) near neutral pH, which suggests that a number of mitochondria from the apoptotic cell population have lost transmembrane potential.

DISCUSSION

Free-flow separation is advantageous in that it does not require the use of gels, which simplifies the procedure and reduces the chance of clogging. Organelle separation in free flow is, however, difficult at larger scale, in part because the high electrical current needed results in heating of the conducting medium. The heating leads to organelle damage and generates density-gradient-driven convections that destroy the resolution of the separation. An efficient cooling system has to be used to alleviate this problem. In contrast, the voltage used in our experiments was about 1000-fold less than what macroscale devices require, resulting in a 1000-fold reduction in the electrical current. Consequently, the power consumed in the microdevice is 10^6 times smaller. Moreover, the

(22) *Product Information: JC-1 and JC-9 Mitochondrial Potential Sensors*; Molecular Probes Inc.: Eugene, OR, 2002.
(23) Reers, M.; Smith, T. W.; Chen, L. B. *Biochemistry* **1991**, *30*, 4480−4486.

large surface area-to-volume ratio of microdevices enhances heat transfer. A simple 2-D (conservative) calculation shows that the temperature rise in our device should be <0.001 °C without active cooling, and there was no observable temperature increase during our experiments.

Another important advantage of miniaturization lies in reducing the time scale of the separation by shrinking the device dimension along which separation occurs ($t \sim L/\mu E$, where L is the width of the channel). Our simulations and experiments have demonstrated that organelles can be concentrated in a few minutes. In addition, the Reynolds number (*Re*) remains small ($\sim 10^{-2}$), so the flow streams are laminar, which should enable the collection of the focused fractions (Figure 1, and see Kenis et al.[24]). The present separation experiments are operated at a large Peclet number ($Pe \sim 10^3$, a measure of convective transport versus diffusive transport), so there is no significant back-diffusion in the direction of the flow. Finally, since the microdevice is operated in continuous mode, the amount of sample processed can be varied for different purposes. Because the total volume of our device is small (2 μL), it is possible to use the device to probe a small population of cells (as few as ~2000 cells in our experiments) for analytical purposes, or it could be optimized for continuous use for larger scale preparatory purposes.

Experiments using the membrane potential-sensitive dye JC-1 show that most mitochondria retain their membrane potential, indicating that the separation process exerts minimal damage to the mitochondria. Furthermore, two distinct subpopulations of mitochondria with differing membrane potential migrate at different pIs. Mitochondria that have lost their membrane potential have a different charge and, in this case, a pI closer to neutral pH. This observation suggests that, with appropriate calibration, the mitochondria fractions with different pIs in IEF could become an assay for the extent of apoptosis for studies.

(24) Kenis, P. J. A.; Ismagilov, R. F.; Whitesides, G. M. *Science* **1999**, *285*, 83−85.

The micro-IEF separation method demonstrated in this work could be applicable to various organelles. Even for organelles that are larger and not as uniform in their pIs, this technique significantly enriches the fraction with the organelles of interest, as shown for nuclei (Figure 6). For organelles (or proteins) that do not possess significantly different pIs (mitochondria and peroxisome, Figure 7), orthogonal methods, such as affinity-based or size-dependent separation, would have to be used in tandem.

CONCLUSION

Using numerical simulations as a guide, we have designed and implemented a microscale organelle separation system. In the microdevices, free flow separation without external cooling is possible because of the almost negligible heat generation and the efficient heat transfer. We have demonstrated rapid, efficient, and procedurally simple separation of mitochondria from intact cells, nuclei, and other cellular debris in the micro-IEF devices. This technique relies on the physiological nature of organelle membranes and maintains the integrity of mitochondria. In a broader context, these devices can also be used to separate other microscale particles based on surface characteristics. The microfabrication techniques implemented here allow flexible designs and potential integration of functions. The microfluidic platform should also facilitate operation of multiple devices in parallel to allow for a large number of simultaneous experiments. When coupled with other modules, these devices could be valuable for data acquisition in cell-based assays for systems biology.

ACKNOWLEDGMENT

We thank DARPA Bio-Info-Micro Program (MDA972-00-1-0030), NIH and NSF graduate fellowship program (to H.L.) for support; the staff of the Microsystems Technology Laboratories at MIT; Prof. P. Sorger for reading the manuscript; L.Y. Koo for supplying NR6wt cells; and R.J. Jackman, J. Voldman, M. Cardone, and J. Elali for helpful discussions.

AC049794G